The Astrophysical Journal, 624:1093–1096, 2005 May 10

SEARCH FOR ACTIVITY IN 3200 PHAETHON

Henry H. Hsieh and David Jewitt
Institute for Astronomy, University of Hawaii, 2680 Woodlawn Drive, Honolulu, HI 96822; hsieh@ifa.hawaii.edu, jewitt@ifa.hawaii.edu
Received 2004 November 29; accepted 2005 January 27

ABSTRACT

We present deep optical imaging of Geminid meteor stream parent 3200 Phaethon taken in search of low-level cometary activity (i.e., coma or dust trail). Although no unambiguous cometary behavior was observed, we find an upper limit on the object's cometary mass-loss rate of $\dot{M}_{\rm lim} \sim 0.01$ kg s^{-1}. The corresponding active fraction (the fraction of the surface area that could consist of freely sublimating water ice) is $f \leq 7 \times 10^{-6}$, at least 2 orders of magnitude smaller than other known comets.

Subject headings: comets: general — meteors, meteoroids — minor planets, asteroids

1. INTRODUCTION

The identification of the Apollo asteroid 3200 Phaethon as the likely parent of the Geminid meteor stream was first made by Whipple (1983) and supported by Gustafson (1989), Williams & Wu (1993), and others. Unlike other meteor stream parents, e.g., 1P/Halley (Orionids), 2P/Encke (Taurids), 55P/Tempel-Tuttle (Leonids), and 109P/Swift-Tuttle (Perseids), Phaethon has never displayed unambiguous cometary activity (e.g., Cochran & Barker 1984; Davies et al. 1984; Chamberlin et al. 1996; Urakawa et al. 2002).

In an effort to shed additional light on this puzzle, we observed Phaethon as the Earth passed through its orbital plane. Dust ejected at low velocity is expected to be confined to the orbital plane; our observations thus maximize the optical depth of any faint coma or trail that may be present. A coma is a common feature of most identified comets. Trails are best known for being seen at infrared wavelengths (Sykes et al. 1986; Sykes & Walker 1992) but have also been optically observed (Ishiguro et al. 2002, 2003; Lowry et al. 2003; Hsieh et al. 2004).

2. OBSERVATIONS

Observations of Phaethon were made in photometric weather on 2003 December 19 using a Tektronix 2048 pixel $\times$ 2048 pixel CCD and a standard Kron-Cousins *R*-band filter at the f/10 focus of the University of Hawaii (UH) 2.2 m telescope on Mauna Kea. Our pixel scale was 0.″219 pixel^{-1}, with seeing of about 0.″8 (FWHM). Because of nonsidereal tracking of the object, background field stars are trailed by $\sim$6″ in our 300 s exposures. During this time, Phaethon had a heliocentric distance of 1.60 AU, a geocentric distance of 1.39 AU, and an orbital plane angle (between the observer and the object orbital plane as seen from the object) of 0.°3.

Standard image preparation (bias subtraction and flat-field reduction) was performed. Flat fields were constructed from dithered images of the twilight sky. Photometry was performed by measuring net fluxes (over sky background) within circular apertures 3.″0 in radius, which were then calibrated to Landolt (1992) standard stars. The mean magnitude (averaged in flux space) of Phaethon during this time was found to be $m_R = 17.12$.

2.1. *Coma Search*

We combined individual images into a single high signal-to-noise ratio composite image (Fig. 1) to search for faint features that would reveal comet-like mass loss. Images were shifted and aligned on Phaethon's photocenter using a fifth-order polynomial interpolation and averaged (excluding maximum and minimum pixel values). We found empirically that this process produced a less noisy profile than median combination. Images were also shifted and aligned on the photocenter of a nearby reference field star.

Each composite image was rotated by 0.°4 clockwise to align the star trails horizontally in the image frame. One-dimensional surface brightness profiles were then obtained by averaging over horizontal rows over the entire widths of the object and reference star and subtracting sky background sampled from either side of the object or star. These profiles were then normalized to unity at their peaks and plotted together (Fig. 2) to search for dissimilarities, particularly an excess in Phaethon's profile, indicating the presence of a coma. We note that some scatter is present in the wings, but we attribute this to a low signal-to-noise ratio far from the nucleus. We thus conclude that no coma is found.

To find quantitative limits, we compared Phaethon's profile with seeing-convolved models of weakly active comets. With the same image scale and point-spread function as our data, these models can be directly compared to the data to ascertain activity levels (Luu & Jewitt 1992). We first created model point sources, then added comae of varying levels, and finally convolved these with the seeing. Coma levels were parameterized by $\eta = C_c/C_n$, where C_c and C_n are the scattering cross-sections of the coma and nucleus, respectively, and the reference photometry aperture radius used was $p = 5.''5$.

To assess the sensitivity of this method, we generated a series of models with coma levels of $\eta = 0.00$–0.05 with $\Delta\eta = 0.01$ (Fig. 3). We see that increasing η has little effect on the profile cores but does broaden the profile wings. We also note that profiles separated by $\Delta\eta = 0.01$ are clearly distinguishable farther than $\sim$2″ from the profile peak. A comparison of these models to Phaethon's measured profile (Fig. 4) produces no indication of activity within our detection limits. We thus find an upper limit on the coma parameter of $\eta \sim 0.01$.

Our limit on η can be converted to a mass-loss rate, $\dot{M}_c$, via

$$\dot{M}_c = \frac{(1.1 \times 10^{-3})\pi\rho\bar{a}\eta_{\rm lim} r_{\rm obj}^2}{pR^{0.5}\Delta} \quad (1)$$

(Luu & Jewitt 1992), where $\rho = 1000$ kg s^{-1} is the assumed grain density, $\bar{a} = 0.5 \times 10^{-6}$ m is the assumed weighted mean grain radius, $r_{\rm obj} = 2350$ m is the object's effective radius (Green

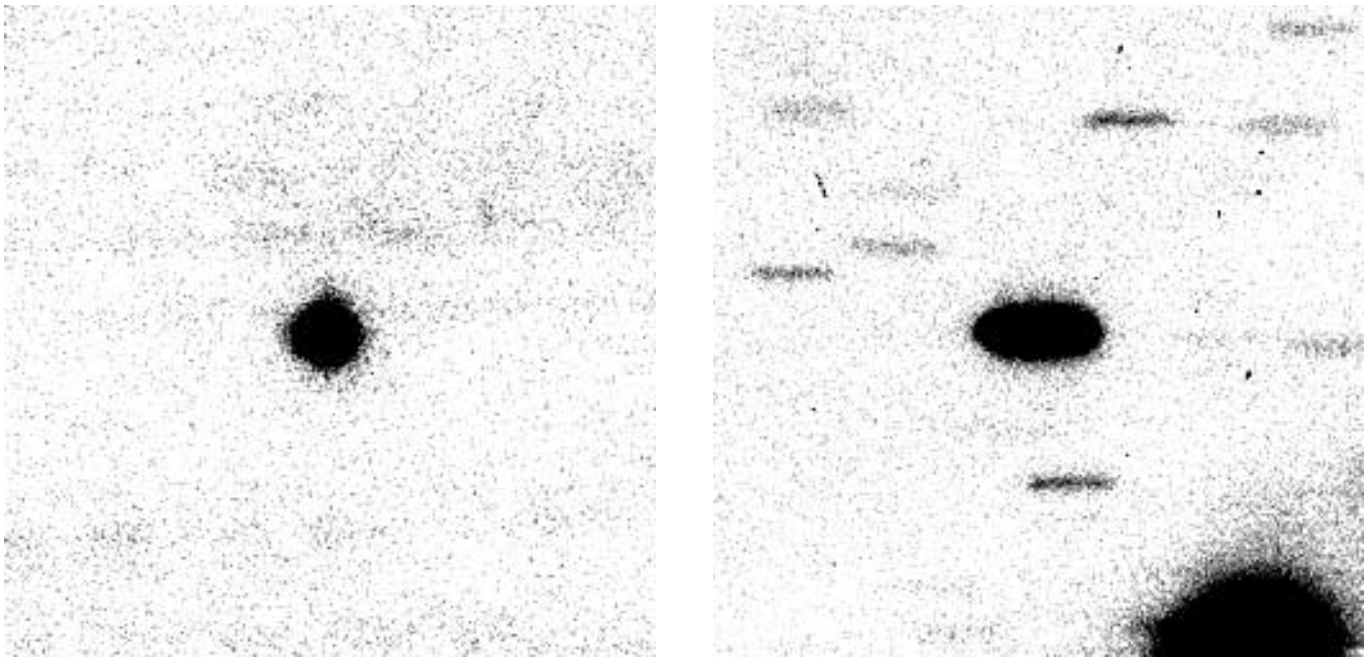

FIG. 1.—Composite *R*-band images of Phaethon (*left*) and a selected reference star (*right*), centered in each frame, constructed from data obtained on 2003 December 19 on the UH 2.2 m telescope. Each image comprises 3600 s in effective exposure time and is 1 arcmin^2, with north at the top and east to the left.

et al. 1985), p is the angular photometry radius in arcseconds, R is the heliocentric distance in astronomical units, and Δ is the geocentric distance in astronomical units. Thus, using $\eta_{\rm lim} \sim 0.01$, we find $\dot{M}_{\rm lim} \sim 0.01$ kg s^{-1}.

We then use $\dot{M}_{\rm lim}$ to estimate a limiting active fraction f of Phaethon's surface from

$$f = \frac{\dot{M}}{4\pi r_{\rm obj}^2 \mu \dot{m}_w}, \qquad (2)$$

where $\mu = 1$ is an assumed dust-to-gas ratio. The mass flux of water (the presumed primary volatile material), $\dot{m}_w$, is computed from

$$\frac{F_\odot(1-A)}{R^2} = \chi\left[\epsilon\sigma T^4(R) + L(T)\dot{m}_w\right], \qquad (3)$$

where $F_\odot = 1370$ W m^{-2} is the solar constant, $A = 0.1$ is the assumed albedo, $\epsilon = 0.9$ is the assumed emissivity, T is the temperature, χ describes the distribution of solar heating over the nucleus surface (ranging from $\chi = 1$ for a flat slab facing the Sun

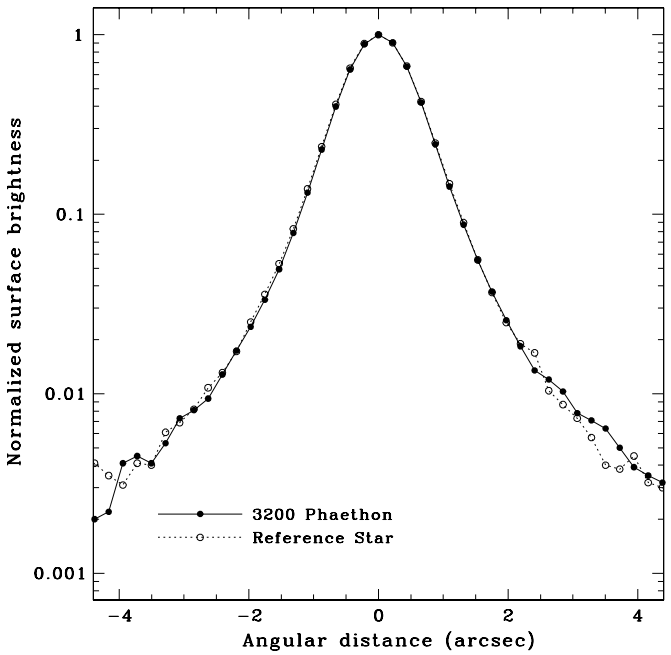

FIG. 2.—Comparison of the surface brightness profiles of the composite images of Phaethon and a reference star. Surface brightness is normalized to unity at each profile's peak and is plotted on a logarithmic scale against angular distance in the plane of the sky.

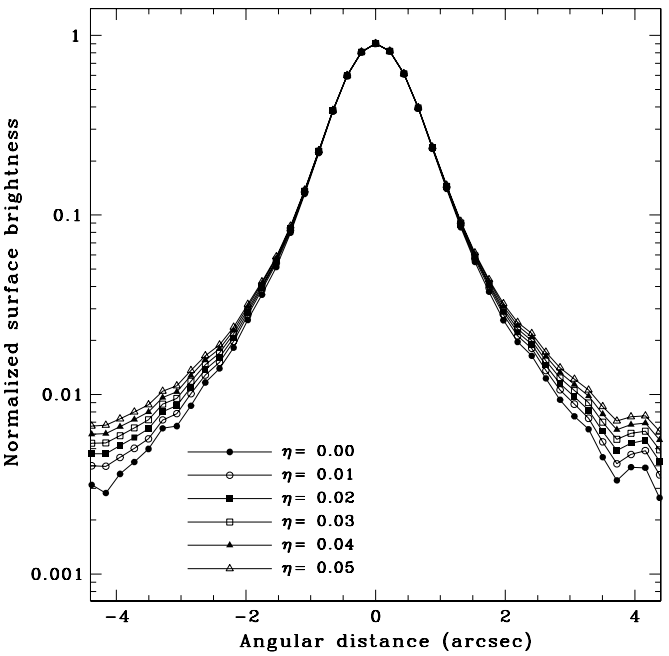

FIG. 3.—Surface brightness profiles of seeing-convolved model nuclei with varying levels of coma ($\eta = 0.00$–0.05).

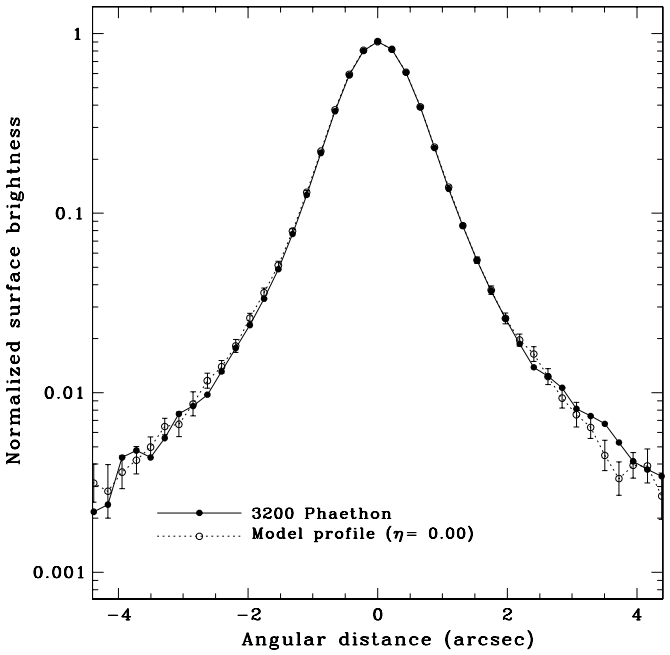

FIG. 4.—Surface brightness profiles of a composite image of Phaethon and a seeing-convolved model nucleus with no coma ($\eta = 0.00$). Error bars indicate uncertainties in η of 0.01 (i.e., the difference between models for $\eta = 0.00$ and 0.01 at each point).

to $\chi = 4$ for an isothermal sphere, as in the case of a fast rotator), and $L(T) = (2.875 \times 10^6) - (1.111 \times 10^3)T$ J kg^{-1} is the latent heat of sublimation for water.

When we solve iteratively, we find mass-loss rates at $R = 1.60$ AU ranging from $\dot{m}_w = 1.47 \times 10^{-4}$ kg m^{-2} s^{-1} for $\chi = 1$ to $\dot{m}_w = 1.96 \times 10^{-5}$ kg m^{-2} s^{-1} for $\chi = 4$. Although Phaethon's 3.60 hr rotation period (Krugly et al. 2002) is quite short, implying that the fast-rotator case ($\chi = 4$) should apply, the possibility that its rotational axis may lie near the ecliptic plane (Krugly et al. 2002) suggests that the slab model ($\chi = 1$) may also apply at certain orientations. If we use the extreme case of an isothermal sphere ($\chi = 4$), we find a maximum active fraction limit of $f \leq 7 \times 10^{-6}$ (using $\chi = 1$ gives $f \leq 1 \times 10^{-6}$). This is an order of magnitude smaller than the smallest active fraction limits found for near-Earth asteroids by Luu & Jewitt (1992) and at least 2 orders of magnitude smaller than fractional active areas found for comets by A'Hearn et al. (1995) and the active area limit ($f \leq 1 \times 10^{-4}$) reported for Phaethon on the basis of spectroscopic observations (Chamberlin et al. 1996).

2.2. *Dust Trail Search*

The dust trail of 133P/(7968) Elst-Pizarro was seen oriented along the object's orbital plane (Hsieh et al. 2004), although no measurable coma was observed. If dust emitted from Phaethon includes a significant component of large ($\gg 1$ μm), low-velocity (~ 1 m s^{-1}) particles, an Elst-Pizarro–like trail could form even in the absence of a detectable coma. To search for such a trail, we rotate the composite image of Phaethon clockwise by 153°.2 to orient the orbital plane horizontally in the image frame (Fig. 5, *left*). In this orientation, any antisolar dust trail should be seen extending to the right of the object. Visual inspection, however, reveals no such trail. For comparison, we also show an image of 133P/(7968) Elst-Pizarro to show how such a feature could appear (Fig. 5, *right*).

We also conducted a quantitative search by measuring the flux contained in adjacent rectangular apertures (4″.4 × 4″.4) extending horizontally on either side of the nucleus, i.e., where any trail should lie. Sky background was sampled using 2″.4 × 4″.4 apertures above and below the trail apertures. The net linear surface brightness is then normalized by dividing by the object's brightness. Uncertainties are derived from rms variations in individual pixels in sky background measurements. The resulting plot (Fig. 6) shows no systematic excess flux to a level of 0.1% of nucleus brightness (equivalent to ~24.6 mag) per linear arcsecond. For comparison, when the trail of 133P/(7968) Elst-Pizarro

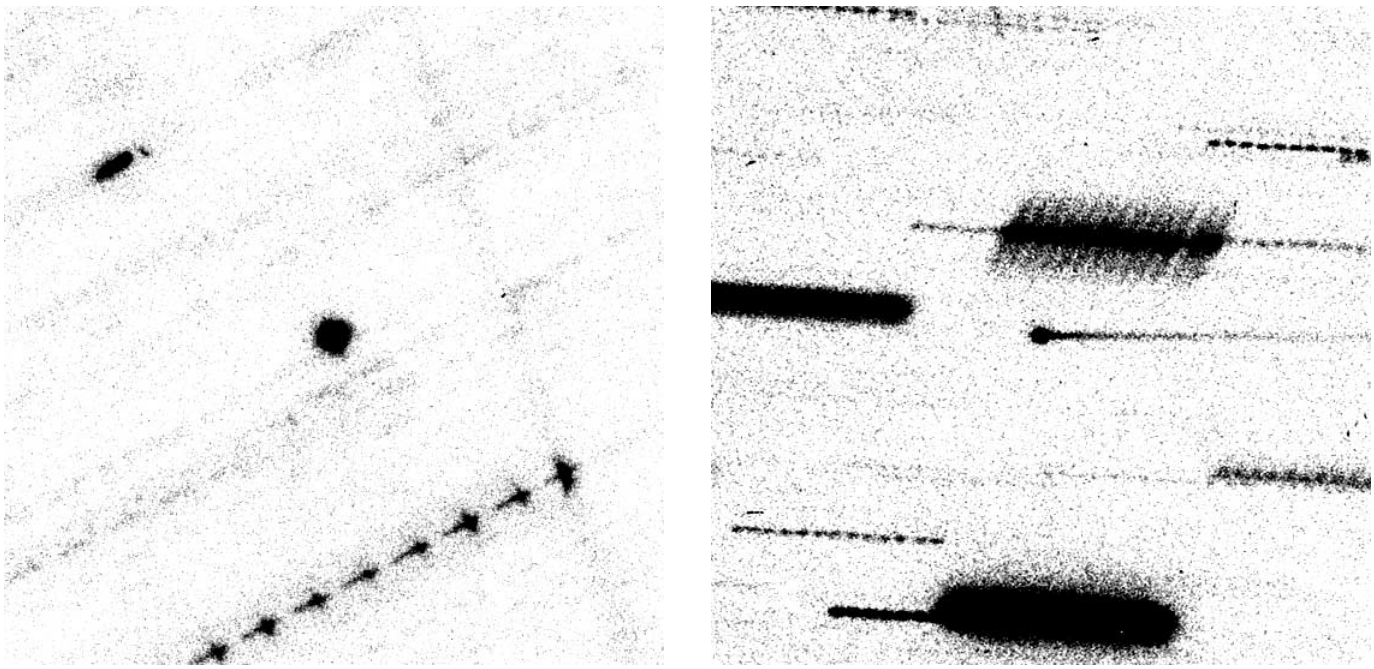

FIG. 5.—Composite *R*-band images of Phaethon (*left*) and 133P/(7968) Elst-Pizarro (*right*), centered in each frame, rotated to orient their orbital planes horizontally in the image frame. The antisolar direction is to the right in each case. The 133P/(7968) Elst-Pizarro image (from 2002 September 7) represents 3900 s of effective exposure time on the UH 2.2 m telescope (Hsieh et al. 2004). Both images are 2′ on each side.

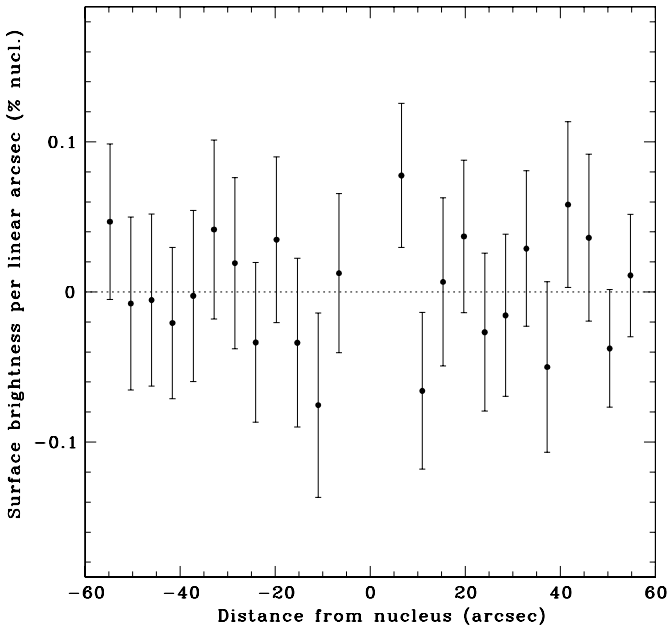

FIG. 6.—Normalized excess surface brightness (over background sky; units in percentage of object brightness per linear arcsecond) along the expected direction of any Phaethon dust trail. The positive *x*-axis denotes distance to the right of the object (as seen in Fig. 5).

was visible, its excess flux was on the order of 1% of nucleus brightness per linear arcsecond, an order of magnitude larger than the limit found here. We conclude that no trail is present.

3. DISCUSSION

Despite its reported dynamical association with the Geminids, we possess no direct physical evidence for Phaethon's cometary nature. Green et al. (1985) inferred from infrared observations that Phaethon may have a rocky, un–comet-like surface, although those same observations indicate that Phaethon is rather atypical for an Apollo asteroid as well. Meanwhile, the bulk density of Geminid meteoroids was found to be particularly high relative to that of other major meteor streams of unambiguous cometary origin (Babadzhanov 2002). Given that the range of surface properties and densities of known comet nuclei are not currently well constrained by available observations, however, these data are inconclusive for ruling out a cometary origin for Phaethon.

Phaethon's current lack of activity does not mean that it has never been or never will be active (e.g., Hartmann et al. 1987). The Geminid meteor stream has been estimated from dynamical considerations to be about 1000 years old (e.g., Williams & Wu 1993), and so current activity is not required to generate presently observed meteors. If we assume a thermal diffusivity of $\kappa = 10^{-6}$ m^2 s^{-1}, the thermal diffusion timescale for Phaethon is $r_{\rm obj}^2/\kappa \sim 2 \times 10^5$ yr, shorter than dynamical lifetimes of 10^6–10^7 yr estimated for similar orbits (e.g., Harris & Bailey 1998). Thus, if we assume thermal equilibration and a semimajor axis of 1.27 AU, Phaethon's average internal temperature is about 250 K, too warm for water ice to survive for very long. This suggests that Phaethon's volatile supply may have been exhausted long ago, particularly in its upper layers. Thermal equilibrium may not apply, however, since Krugly et al. (2002) report a spin axis orientation close to the ecliptic plane for Phaethon, suggesting that heating and therefore activity from an isolated volatile patch could be seasonally modulated. If so, monitoring for cometary behavior should be continued as far around the orbit as possible. Phaethon's true nature must still be considered an open question.

We thank Scott Sheppard for donated observing time and NASA for support of this work through a grant to D. J.

REFERENCES

A'Hearn, M. F., Millis, R. L., Schleicher, D. G., Osip, D. J., & Birch, P. V. 1995, Icarus, 118, 223
Babadzhanov, P. B. 2002, A&A, 384, 317
Chamberlin, A. B., McFadden, L., Schulz, R., Schleicher, D. G., & Bus, S. J. 1996, Icarus, 119, 173
Cochran, A. L., & Barker, E. S. 1984, Icarus, 59, 296
Davies, J. K., Green, S. F., Stewart, B. C., Meadows, A. J., & Aumann, H. H. 1984, Nature, 309, 315
Green, S. F., Meadows, A. J., & Davies, J. K. 1985, MNRAS, 214, 29P
Gustafson, B. Å. S. 1989, A&A, 225, 533
Harris, N. W., & Bailey, M. E. 1998, MNRAS, 297, 1227
Hartmann, W. K., Tholen, D. J., & Cruikshank, D. P. 1987, Icarus, 69, 33
Hsieh, H. H., Jewitt, D. C., & Fernández, Y. R. 2004, AJ, 127, 2997
Ishiguro, M., Kwon, S. M., Sarugaku, Y., Hasegawa, S., Usui, F., Nishiura, S., Nakada, Y., & Yano, H. 2003, ApJ, 589, L101
Ishiguro, M., et al. 2002, ApJ, 572, L117
Krugly, Y. N., et al. 2002, Icarus, 158, 294
Landolt, A. U. 1992, AJ, 104, 340
Lowry, S. C., Weissman, P. R., Sykes, M. V., & Reach, W. T. 2003, Lunar Planet. Sci. Conf., 34, 2056
Luu, J. X., & Jewitt, D. 1992, Icarus, 97, 276
Sykes, M. V., Lebofsky, L. A., Hunten, D. M., & Low, F. 1986, Science, 232, 1115
Sykes, M. V., & Walker, R. G. 1992, Icarus, 95, 180
Urakawa, S., Takahashi, S., Fujii, Y., Ishiguro, M., Mukai, T., & Nakamura, R. 2002, in IAU Colloq. 181, Dust in the Solar System and Other Planetary Systems, ed. S. F. Green, I. Williams, T. McDonnell, & N. McBride (Amsterdam: Pergamon), 83
Whipple, F. L. 1983, IAU Circ., 3881, 1
Williams, I. P., & Wu, Z. 1993, MNRAS, 262, 231